C.P. No. 7
(12,390)
A.R.C. Technical Report

MINISTRY OF SUPPLY

AERONAUTICAL RESEARCH COUNCIL

CURRENT PAPERS

Report on Measurements of the Pressure Distribution over a Wing of Triangular Plan Form at a Mach Number of 2.44

By

G. H. Lean, B Sc, B Sc., D.I.C. and K. G. Whitaker, G. I. Mech. E.
of the Engineering Division, N.P.L.

LONDON : HIS MAJESTY'S STATIONERY OFFICE

1950

Price 1s. 0d. net.

Engineering Division Report No. Eng.Divn. 357/48

Report on Measurements of the Pressure Distribution over a Wing of Triangular Plan Form at a Mach Number of 2.44

- by -

G.H. Lean, B.Sc., DIC and K.G. Whitaker, G.I.Mech.E.

Communicated by Superintendent, Engineering Division, N.P.L.

July, 1948

1. Summary:

The pressure distribution over the surfaces of a wing of triangular plan form with apex angle less than the Mach angle and of simple wedge section $6\frac{1}{2}$" thick has been measured in the 11 inch square supersonic tunnel. The integrated force coefficients have been compared with calculations based on the linearised equation for thin flat delta wings. It is found that while the lift coefficients are in close agreement, the induced drag coefficients are considerably greater than those calculated. As might be expected the agreement is much better if the term associated with the occurrence of infinite suction on the leading edge is excluded, for the pressures close to the leading edge could not be explored due to the small thickness.

At zero incidence the pressure drag on the sides of the wing is somewhat higher than that calculated for the front half of a diamond shaped aerofoil of similar apex and section angle. The difference is attributed to lack of uniformity in the approaching flow and to flow in the boundary layer at the wing root.

An estimate of skin friction drag indicates that the contribution from this cause is about double the pressure drag on the sides at zero incidence.

2. Introduction

The experiments to be described were instituted mainly to provide preliminary data which could be used subsequently to compare with similar measurements over wings of other shapes. The model used was not designed initially for the present purpose and its construction imposed limits on the position of the pressure holes which rendered the measurements somewhat unsuitable for comparison with the results of calculation.

3. Description of Model

The model (span $4^1/8$", root chord $10^1/8$") was approximately triangular in plan form, the leading and trailing edges being inclined at angles of $20\frac{3}{4}^\circ$ and 74° to the wind direction respectively (Fig.1.) The Mach angle of the incident flow was about 24°, so that the leading edge fell inside the Mach cone from the apex.

The model was open at the rear, its surfaces being made of two steel plates inclined to one another at a constant angle which were soldered together along the leading edge and finished knife sharp, thus the sections parallel to the wind direction were triangular.

4. Description of Tests

The model was bolted to a brass turntable which was mounted on the tunnel with its surface flush with the inside. A small clearance was left between the root chord of the model and the side, so that it could be rotated while the tunnel was running. A slot cut in the turntable communicated with the inside of the model so that air could be bled out of the rear of the model if required.

A number of pressure holes were drilled through the model surfaces at the points marked in Fig. 1 and connected with steel tubes soldered to the inside. The tubes were led through the side of the turntable through a vacuum tight gland, each being connected to the column of a mercury multi-tube manometer.

Throughout the tests the pressure and temperature at inlet to the tunnel was maintained constant, the Reynolds number $(\frac{Uc}{\nu})$ based on the maximum chord being 0.94×10^6.

The zero incidence position was determined by turning the model until the pressure at a hole in the upper surface was equal to the mean of the pressures at holes symmetrically situated with it on the lower surface.

Since the model was symmetrical the pressures on a single surface at equal positive and negative incidences could be used to give the pressures on the two surfaces.

5. Preliminary Tunnel Exploration

Before making measurements on the model, the pitot and static pressure distributions were determined in the empty tunnel in planes $\frac{1}{2}$" above and below the position occupied by the model (Fig.2). The presence of pressure gradients may be expected to distort the pressure distribution over the model, although in the case of the lift component the errors on each surface may tend to cancel. No account has been taken of the non-uniformity in the flow in the evaluation of the forces, the Mach number and pressure being assumed equal to the mean values approaching the wing.

Recent measurements of pitot and static pressures in the boundary layer on the tunnel wall in the empty tunnel showed that the velocity began to fall away from the main stream value at about 0.6" from the wall, the displacement thickness being 0.12" near the position occupied by the leading edge of the model. No measurements of pressure and velocity have been taken near the wall with the model in position and the force coefficients have been based on the pressure distribution over the outer 75% of the span. The direct effect of boundary layer on the coefficients have not therefore been included.

6. Results of Tests

The pressure distributions over the model surfaces for incidences of 0, $2\frac{1}{2}^\circ$, 5°, $7\frac{1}{2}^\circ$ and 10° are shown in Fig. 3 where the results are plotted as isobars. It will be noticed that in general the pressures tend to increase or decrease towards the leading edge, according to whether the slope of the surface is positive or negative. (The slope is taken as positive when the surface is inclined towards the stream, e.g. the lower surface).

The force coefficients and centre of pressure positions derived from the pressure integrations over the upper and lower surfaces are given in Table 1. The tabulated coefficients are defined in the usual way e.g., the drag coefficient is evaluated from $D = \int (p - p_s) dS$; $C_{D_S} = \frac{D}{\frac{1}{2}\rho U^2 S}$ where S is the plan area of the wing; p_s, ρ and U being the mean pressure, density and velocity of the approaching stream and p, dS are the pressure and directed area of the surface in the drag direction respectively.

Table 1/

Table 1. Force Coefficients and Centres of Pressure Positions Over Sides of Model

Incidence	0°	2½°	5°	7½°	10°
Drag Coefficient (C_{D_s})	.0022	.0045	.0142	.0289	.0508
Lift Coefficient (C_L)	0	.0579	.1470	.2074	.279
* Lateral Force Coefficient (Cy)	.036	.036	.028	.023	.017
Lift/Drag	0	12.9	10.3	7.2	5.5
Perpendicular Distance from centre of pressure to Leading Edge as fraction of span (3 1/8").	0.31	0.27_5	0.26	0.27	0.29
Perpendicular Distance from centre of pressure to Trailing Edge as Fraction of span (3 1/8").	0.76	0.79	0.75	0.76	0.75

* Lateral Force positive when directed towards the root.

It is evident from the table that the lift/drag ratio rises steeply to a maximum at about 2½° incidence and then falls more slowly. These ratiostogether with the lift and drag coefficients are plotted in Fig. 4.

At zero incidence the centre of pressure was about 3½% of the span behind the centroid of the surfaces (30 and 80% of the span from the leading and trailing edges respectively).

During the tests the pressure inside the wing (corresponding to the pressure (p_b) at the base of the model) was measured. The ratio of this pressure to the mean static pressure in the free stream is given in the following table, together with the overall pressure drag coefficient.

Table 2. Base Pressure and Total Pressure Drag Coefficient (C_D)

Incidence	0°	2½°	5°	7½°	10°
Ratio of base to static pressure.	0.43	0.39	0.37	0.36	0.33
Base Drag Coefficient(C_{Db})	.0088	.0095	.0097	.0100	.0104
Pressure Drag Coefficient ($C_{Ds} + C_{Db}$)	.0110	.0140	.0239	.0389	.0612

It is evident that at zero incidence the drag due to the suction at the base is four times the pressure drag over the sides of the model. However, although the base drag increases with incidence, the increase is much less rapid than that over the sides, the contributions being approximately the same at an incidence of about 4°.

It may be of interest to mention that during one test, air was led into the inside of the model through the turntable sufficient to raise the internal pressure to $2\frac{1}{2}$ times the static pressure. Up to this value, with the model at zero incidence, the pressures at the last row of holes (situated 0.17" upstream of the trailing edge) were not sensibly affected.

7. Discussion

In Ref. 1, the pressure distribution for a wing of diamond shaped plan form of double wedge section (semi angle β) at zero incidence has been derived from the linearised theory for wings of small thickness-chord ratio. The calculated pressure distribution over the front part of such a wing, for the same ratio of apex to Mach angle as the model, has been compared with the measured distribution (Fig. 5). While the pressures are of the same order as those predicted by the theory, the shape of the isobars is quite different, and the measured drag coefficient for the sides of the model (.0022) is considerably greater than that calculated (.0016). This difference is mainly attributed to lack of uniformity in the flow approaching the model and possibly to secondary causes due to the flow in the boundary layer at the wing root.

It is of some interest to use the base pressure measurements to compare the drag coefficient of the delta shaped wing with that of diamond plan form. Thus taking the above calculated figure for the drag coefficient and adding the drag contribution from the base, a value (.0104) is obtained which is only 17% higher than that for a diamond aerofoil of the same angle of sweep back and thickness/chord ratio. Thus it might be said that the advantage of streamlining is almost wholely offset by the reduction of nose angle. Expressions for the lift and induced drag coefficients for a thin flat delta wing with apex semi angle less than the Mach angle are given in References 2 and 3. They are

$$C_L = \frac{2\pi\alpha \tan y}{E'} \qquad \ldots\ldots\ldots (1)$$

$$\text{and } C_{D_i} = \frac{1}{4\pi \tan y}\left[2E' - \sqrt{1 - \frac{\tan^2 y}{\tan^2 \mu}}\right] C_L^2 \qquad \ldots\ldots\ldots (2)$$

where α = incidence (radians)

y = semi apex angle

μ = Mach angle

and E' = Complete elliptic integral of the second kind to modulus

$$\sqrt{1 - \frac{\tan^2 y}{\tan^2 \mu}}\ .$$

In the expression (2) for the induced drag, defined as the drag associated with lift, the first term on the right hand side represents the resultant of the pressures over the surfaces in the drag direction. The second negative term is due to the occurrence of infinite suctions on the leading edge. For the present model the two terms become

$$C_{D_i} = \left[.61 - .11 \right] C_L^2 = .50 \, C_L^2$$

For comparison, the difference of the measured drag over the sides of the model and that at zero incidence has been plotted against the square of the left coefficient - (Fig. 6). The plotted points lie approximately on the straight line $C_{D_i} = 0.62 \, C_L^2$.

The agreement of the experimental results with the theoretical values when the second term is excluded is striking. The presence of high suctions at the leading edges would not be revealed in the present tests since the pressure holes could not be positioned closer than $\frac{1}{2}$" to the leading edge.

In the experiments, no measurements of the drag due to skin friction were made. An indication of the contribution from this factor is given by recent boundary layer measurements on the tunnel wall. These were made at a Reynolds number of about 2×10^6 and gave a friction coefficient (C_f) about .0023. Taking this value as applicable to the present model, the friction drag coefficient is .0046, i.e. about twice the pressure drag on the sides of the model at zero incidence. Making a similar allowance at other incidences the drag coefficients and lift/drag ratios are given in the following table.

Table 3. Drag Coefficients and Lift/Drag Ratios for Model

Incidence	0°	$2\frac{1}{2}$°	5°	$7\frac{1}{2}$°	10°
Drag Coefficient for Sides of Model	.0068	.0091	.0188	.0335	.0554
Total Drag Coefficient (including base suction).	.0156	.0186	.0285	.0435	.0658
Lift/Drag (Sides of Model)	0	6.4	7.8	6.2	5.0
Lift/Drag (Total)	0	3.1	5.2	4.8	4.2

8. Conclusion

The pressure distributions over the sides of the model differ considerably from those which would be expected from the linearised theory giving a higher drag at zero incidence than the calculated value. These discrepancies may be attributed to lack of uniformity in the flow approaching the model and to secondary causes due to the flow in the boundary layer at the wing root.

While the lift coefficients agree closely with those calculated for the flat delta wing, the measured induced drag coefficients are somewhat higher. However, the theoretical expression for the latter includes a term associated with the presence of infinite suctions on the leading edge. In the tests, because of the small thickness, the pressures close to the leading edge could not be measured and if the theoretical term just referred to is excluded much better agreement is obtained.

The/

The overall pressure drag on the model at zero incidence is about 17% higher than the calculated value for a diamond shaped aerofoil of the same apex angle and thickness/chord ratio.

Measurements of skin friction on the sides of the tunnel indicate that the drag from this cause is considerable, being about twice the pressure drag on the sides of the model at zero incidence.

9. References

1. Wave Drag of an Aerofoil at Zero Incidence
A. Robinson, R.A.E. Report No. Aero 2159. A.R.C. 10,311.

2. Aerofoil Theory of a Flat Delta Wing at Supersonic Speeds
A. Robinson, R.A.E. Report No. Aero 2151. R. & M. 2548.

3. Supersonic Aerodynamics - principles and applications
T. Von Karman, J.Aero.Sci. July '47, Vol. 14.

National Physical Laboratory,
6th May, 1948
Eng/55C/DI

ENG DIV. 357/48

FIG. 1.

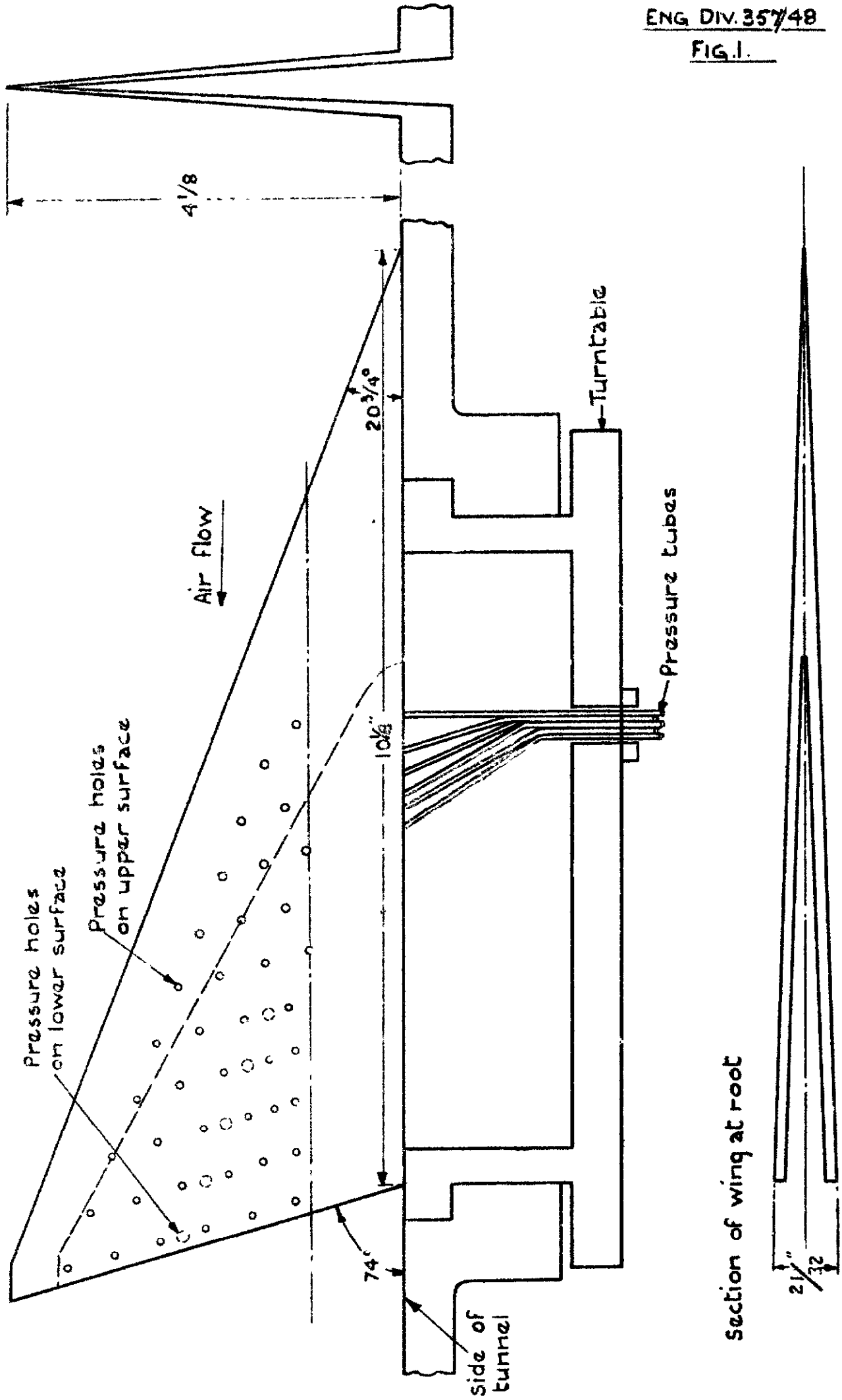

Fig 1. Arrangement of Wing Mounted on Turntable

AUG 1948, NATIONAL PHYSICAL LABORATORY, ENG. DIVISION

C160/108

Fig 2. Pressure and Mach Number Distribution in Empty Tunnel at Position Occupied by Model

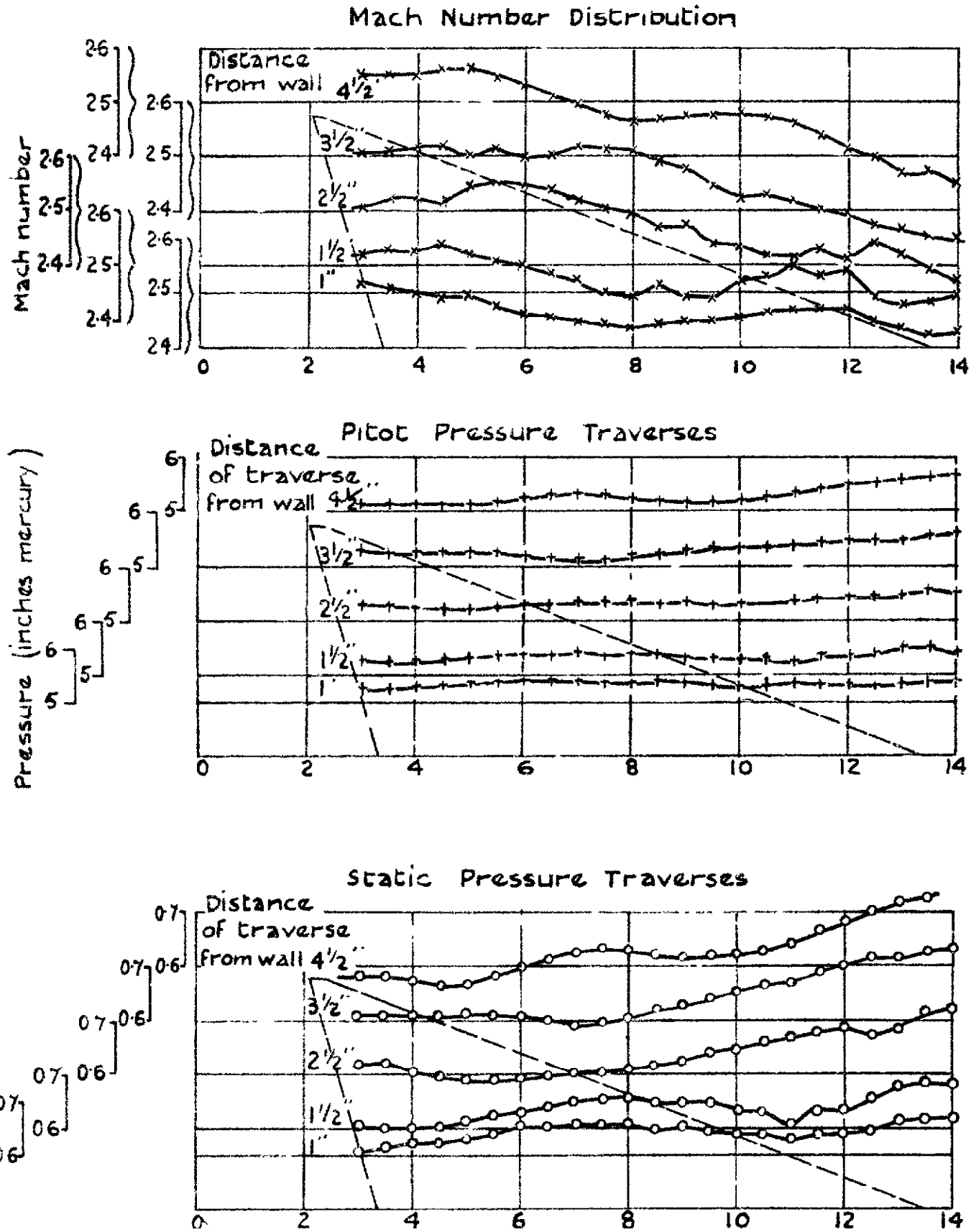

Fig. 3. Pressure Distribution over Sides of Model

The figures marked on isobars are values of $\frac{\Delta p}{\frac{1}{2}\rho V^2}$

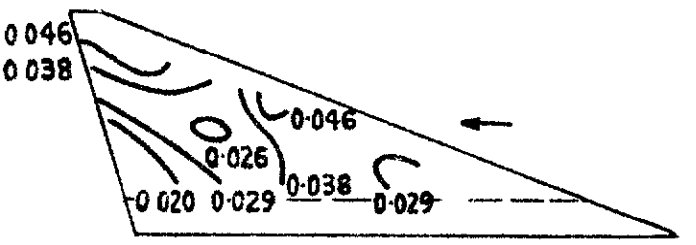

0° Incidence

Upper Surface

Lower Surface

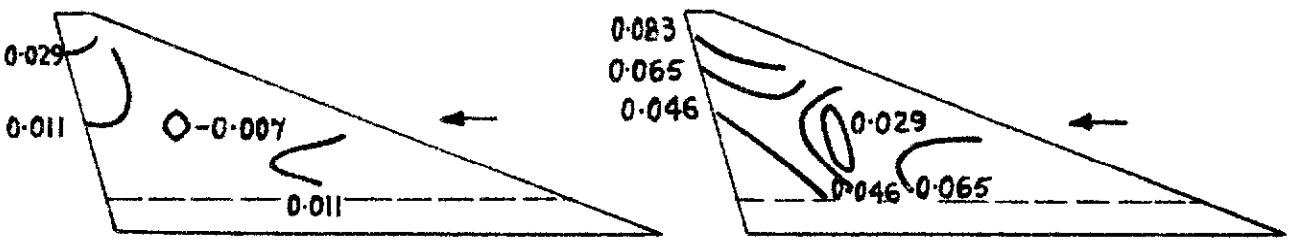

2·5° Incidence

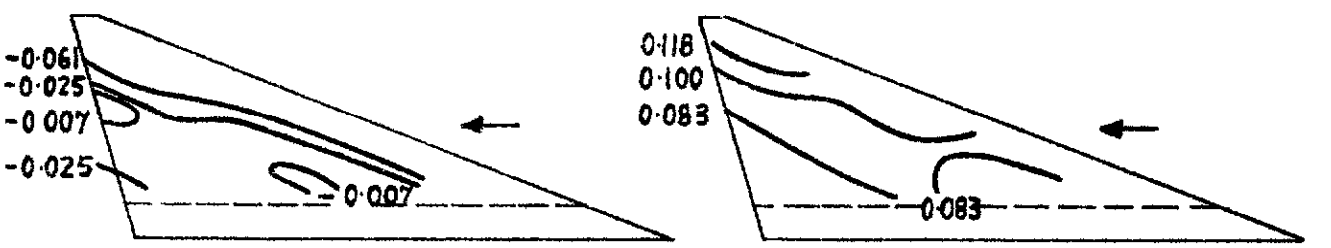

5° Incidence

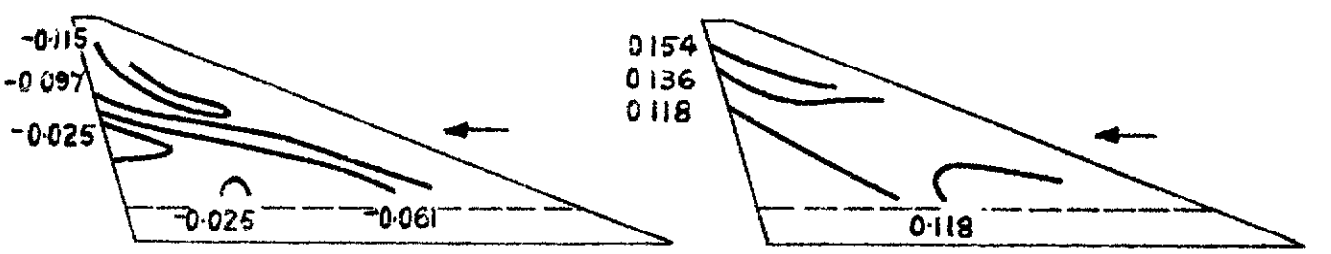

7·5° Incidence

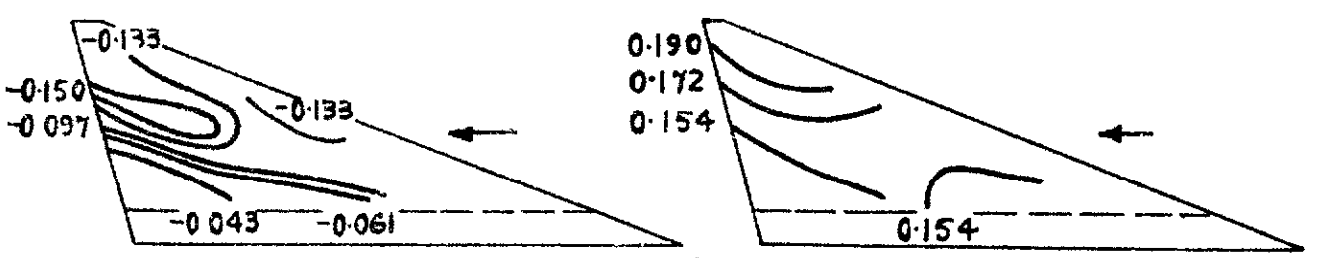

10° Incidence

Fig 4. Lift and Drag Coefficients over Sides of Model.

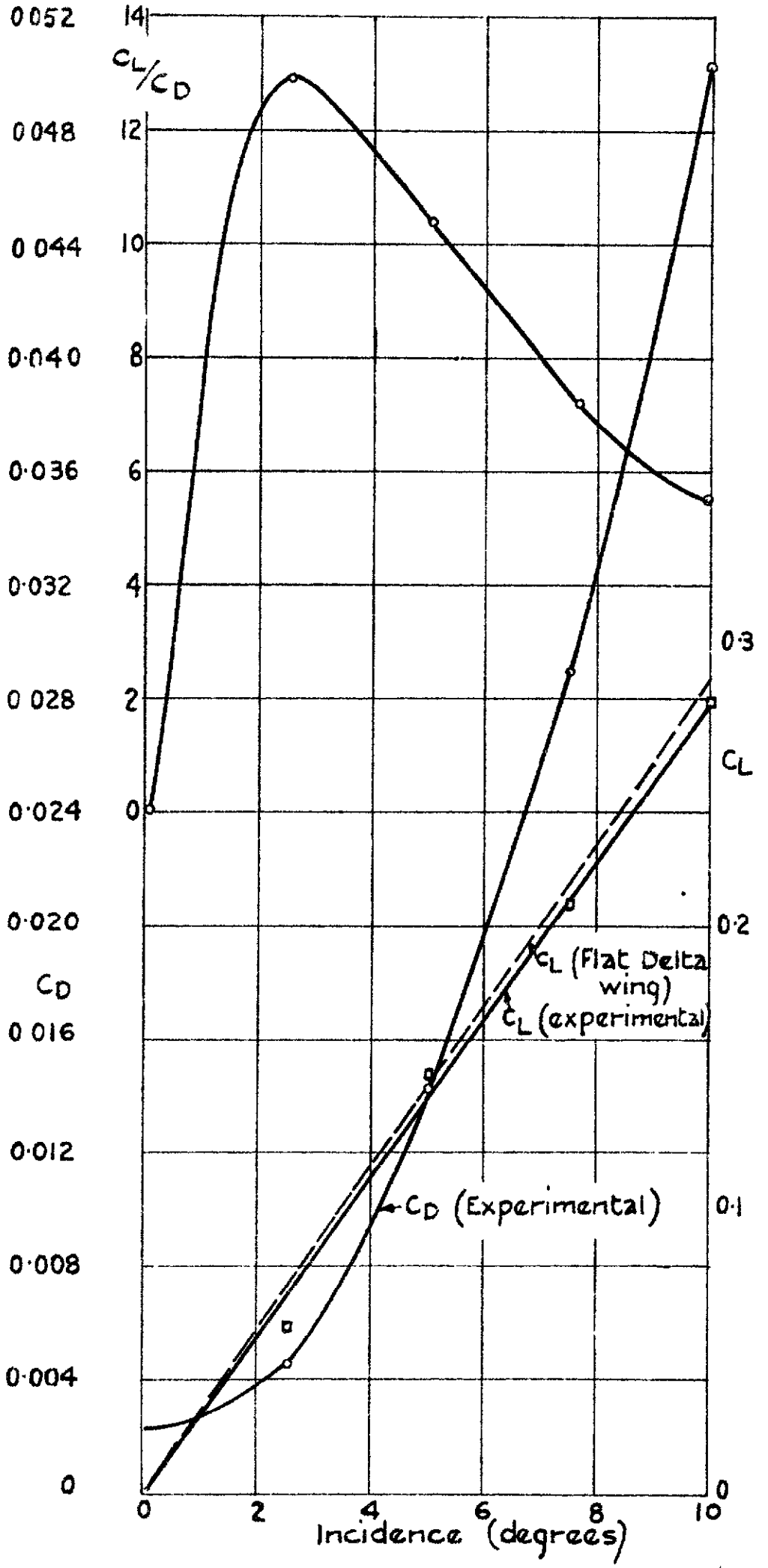

Fig. 5 Comparison of Calculated and Experimental Pressure Distribution at Zero Incidence
The calculated isobars are shown dotted
The figures marked on curves are values of $\frac{\Delta P}{\frac{1}{2}\rho V^2}$

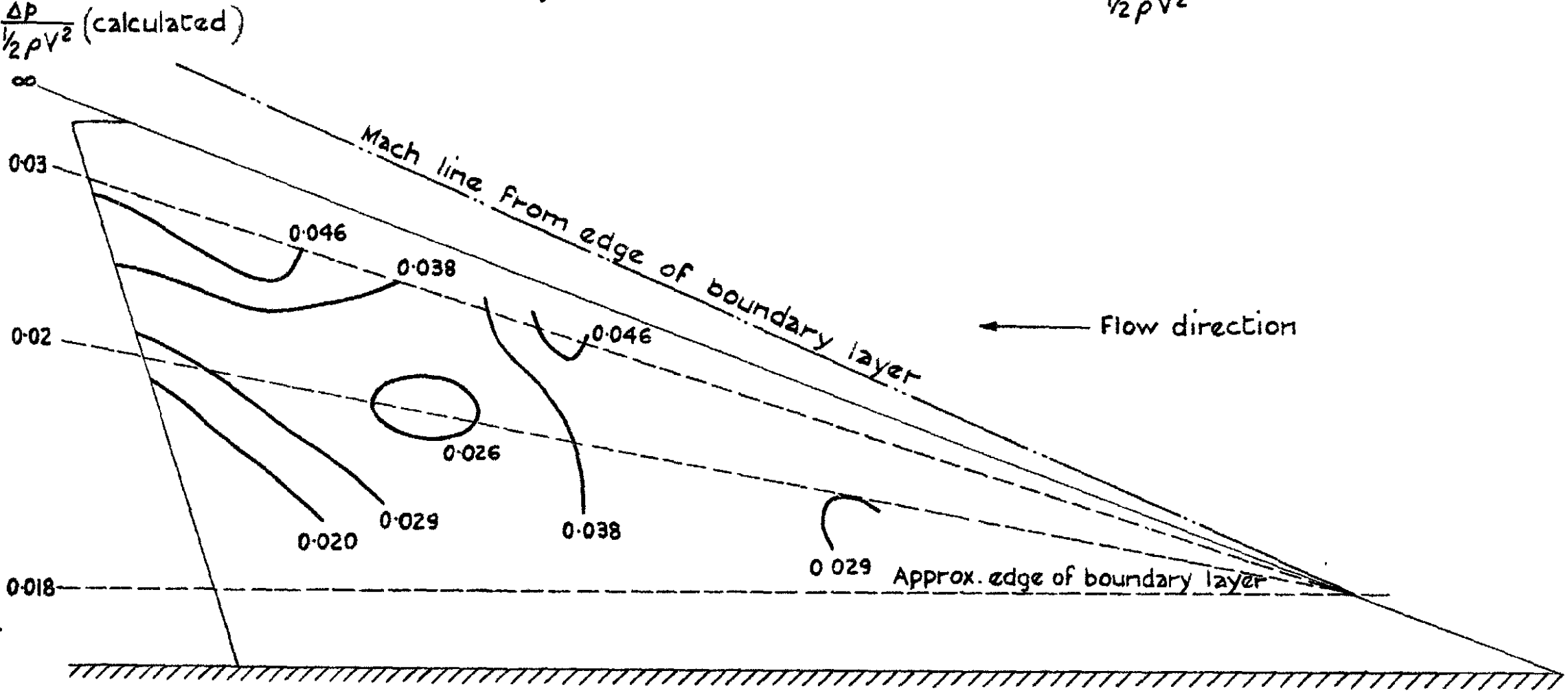

AUG. 1948. NATIONAL PHYSICAL LABORATORY, ENG. DIVISION.
C160/112
ENG. DIV. 35/7/48 FIG. 5.

Fig. 6. Variation of Induced Drag with Lift.

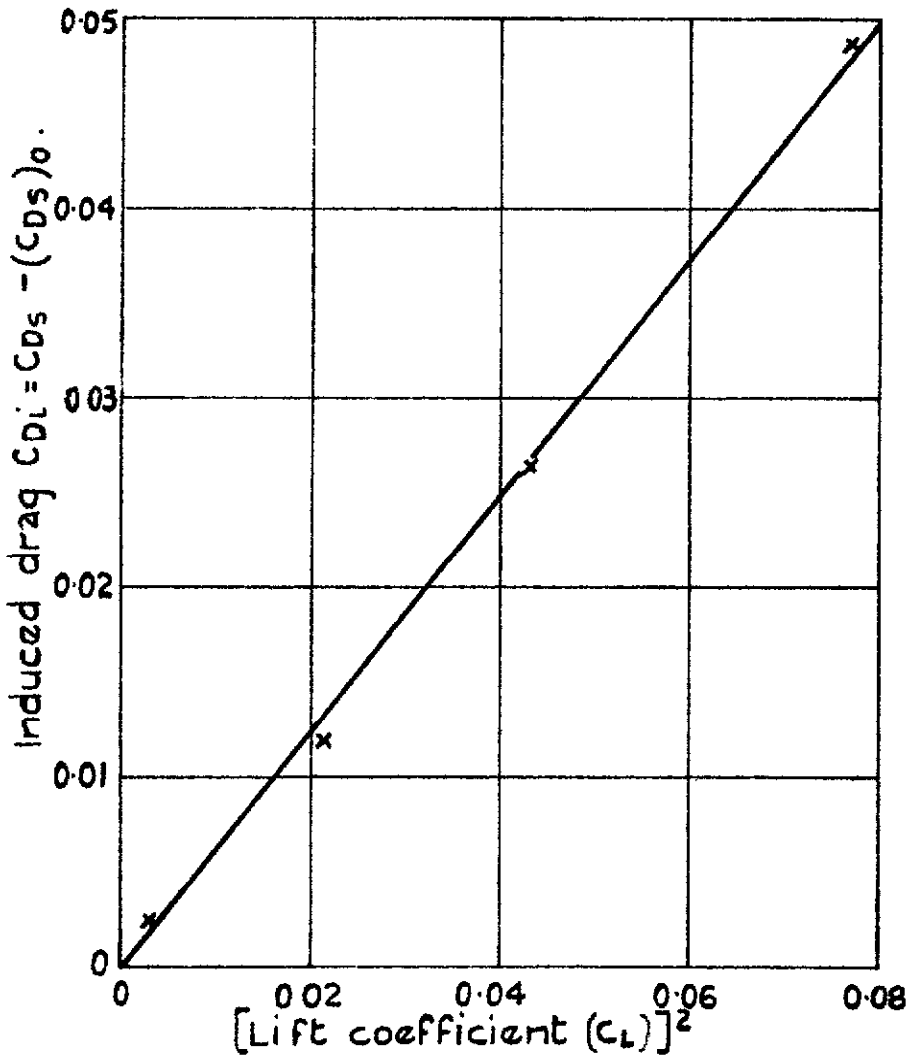

C.P. No 7
(12,390)
A.R C. Technical Report

PUBLISHED BY HIS MAJESTY'S STATIONERY OFFICE
To be purchased from
York House, Kingsway, LONDON, W C 2 429 Oxford Street, LONDON, W I
P.O. Box 569, LONDON, S E I
13a Castle Street, EDINBURGH, 2 I St. Andrew's Crescent, CARDIFF
39 King Street, MANCHESTER, 2 I Tower Lane, BRISTOL, I
2 Edmund Street, BIRMINGHAM, 3 80 Chichester Street, BELFAST
or from any Bookseller
1950
Price 1s. od. net

S.O. Code No. 23-9006-7

D S 39464/K3 (C)